Energy input from the exterior cusp into the ionosphere: Correlated ground-based and satellite observations

E. Yordanova,[1] D. Sundkvist,[2] S. C. Buchert,[1] M. André,[1] Y. Ogawa,[3] M. Morooka,[1] O. Margithu,[4,5] O. Amm,[6] A. N. Fazakerley,[7] and H. Réme[8]

Received 29 October 2006; revised 12 December 2006; accepted 11 January 2007; published 20 February 2007.

[1] The energy transport from the exterior cusp into the ionosphere is investigated using coordinated ground-based (EISCAT and MIRACLE) and satellite (Cluster) observations. EISCAT and MIRACLE data are used to estimate the plasma heating in the *F*-region and the Joule heating in the *E*-region. Cluster measurements are used to derive the electromagnetic and particle energy fluxes at the high altitudes. These fluxes are then compared with the energy deposition into the ionospheric cusp during a 30 minutes long time interval in which Cluster and EISCAT are nearly conjugated. It is shown that the particles seen at about 9 R_e in the exterior cusp carry an earthward energy flux that corresponds to the observed heating of the *F*-region. The estimated earthward Poynting flux is more than enough to account for the Joule heating in the *E*-region.
Citation: Yordanova, E., D. Sundkvist, S. C. Buchert, M. André, Y. Ogawa, M. Morooka, O. Margithu, O. Amm, A. N. Fazakerley, and H. Réme (2007), Energy input from the exterior cusp into the ionosphere: Correlated ground-based and satellite observations, *Geophys. Res. Lett.*, *34*, L04102, doi:10.1029/2006GL028617.

1. Introduction

[2] The energy coming from the solar wind is deposited in the magnetosphere-ionosphere-thermosphere system through electromagnetic energy flux and particle precipitation. The cusp is a key region for the energy input into the system because of the direct access of the solar wind plasma to the magnetosphere and ionosphere. It links high altitude areas adjacent to the magnetosheath, magnetopause, dayside plasma sheet and plasma mantle to the low altitude ionosphere and thermosphere. The exterior cusp is characterized by low magnetic field intensity and stagnant and turbulent magnetosheath plasma [*Dunlop et al.*, 2005; *Lavraud et al.*, 2005]. The low altitude ionospheric cusp has much higher magnetic field intensity due to the magnetic (dipole) field convergence. In the altitude range 300–500 km, the European incoherent scatter (EISCAT) radar recognizes the cusp signatures in terms of enhanced electron density ($\sim 10^{12}$ m^{-3} and more), enhanced electron temperature ($\sim$6000 K) and enhanced ion temperature ($\sim$5000 K) [*Nilsson et al.*, 1996].

[3] Coordinated satellite and ground-based observations are of great importance for understanding the processes of electrodynamic mapping from the solar wind to the magnetosphere and ionosphere. Valuable contributions to our knowledge of magnetospheric physics have been achieved by cooperative research performed by the four Cluster satellites [*Escoubet et al.*, 1997] and ground-based instruments [*Amm et al.*, 2005, and references therein]. The Cluster spacecraft are equipped with state-of-the-art instruments for measuring electric and magnetic fields (EFW and FGM) as well as for detecting the velocity distributions of electrons and ions (PEACE and CIS). Incoherent scatter radars are a very powerful ground-based remote-sensing technique, in particular, the flow of electromagnetic energy as well as the energy of electrons and ions can be relatively reliably derived. Complementary ground-based electrodynamic information is provided by the two-dimensional network Magnetometers-Ionospheric Radars-All-sky Cameras Large Experiment (MIRACLE) [*Syrjäsuo et al.*, 1998].

[4] It is believed that the dominating source of energy input into the cusp *F*-region is the precipitating magnetosheath particles that cause heating via collisions. EISCAT observes heating due to soft (<500 eV) particle precipitation which is usually accompanied by up-welling of the air in the thermosphere. The CHAMP satellite detects up-welling air in each of its crossings of the cusp region [*Lühr et al.*, 2004]. A statistical study based on DE-2 satellite data reveals significant enhancement of the electron temperature in the upper ionospheric cusp (300–800 km) due to soft particle precipitation depending on geomagnetic activity level, season and invariant latitude [*Prölss*, 2006]. Using optical and radio instruments [*Walker et al.*, 1999] show that soft particle precipitation in the *F*-layer above 78° geographic latitude, plays a direct role in the creation of the enhanced electron densities with characteristics of polar cap patches. Similar transient poleward-moving events of elevated plasma density caused by the precipitation of low energy electrons (10–20 eV) at 400–700 km, were observed by simultaneous satellite and ground-based measurements [*Lockwood et al.*, 2001]. Observations by DE 2 in the cusp/cleft region at 400 km, was used to estimate the Joule and particle (electrons with energy <100 eV) heating. It was found that the Joule heating has its maximum at $\sim$120 km, and the particle heating maximizes at $\sim$260 km altitude [*Wu et al.*, 1996]. Here we investigate if the earthward particle energy flux is high enough to explain the ionospheric heating.

[1] Swedish Institute of Space Physics, Uppsala, Sweden.
[2] Space Sciences Laboratory, University of California, Berkeley, California, USA.
[3] National Institute of Polar Research, Tokyo, Japan.
[4] Institute of Space Sciences, Bucharest, Romania.
[5] Also at Max-Planck-Institut fur extraterrestrische Physik, Garching, Germany.
[6] Finnish Meteorological Institute, Geophysical Research, Helsinki, Finland.
[7] Mullard Space Science Laboratory, Dorking, UK.
[8] Centre d'Etude Spatiale des Rayonnements, Toulouse, France.

0094-8276/07/2006GL028617

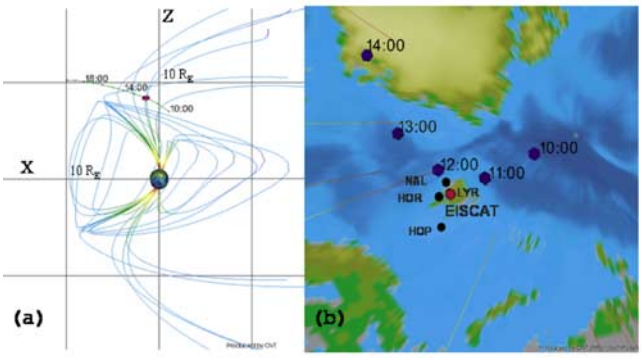

Figure 1. (a) Cluster position (magenta rectangle) in the Tsyganenko 2001 terrestrial magnetic field model (available at http://ovt.irfu.se). (b) Cluster magnetic footprints (blue hexagons) on a map of the high-latitude northern hemisphere with the location of the EISCAT Svalbard radar (red dot) and MIRACLE magnetometers at the ground-based stations NAL, LYR, HOR, and HOP (black dots). The shortest separation between EISCAT and the Cluster footprint is about 400 km at around 12:00 UT.

[5] This case study aims also to elucidate the question whether the observed Poynting fluxes in the exterior and ionospheric cusp are comparable in magnitude. To our knowledge there are very few studies regarding conjunction (high altitude—low altitude—ground-based) events of energy deposition in the cusp and none of them estimates the energy input locally in the lowest ionospheric altitudes. A comparison of the wave Poynting flux and particle energy flux during a Cluster/FAST conjunction event [*Chaston et al.*, 2005], shows that the energy deposition into the dayside auroral oval results in field-aligned electron acceleration, transverse ion acceleration and Joule heating. Iridium/DMSP observations over the region poleward of 78° MLAT during strong northward interplanetary magnetic field (IMF), give an estimation of eight times larger electromagnetic energy input into the ionosphere than the energy input due to particle precipitation [*Korth et al.*, 2005].

[6] We use conjugate Cluster, EISCAT and MIRACLE observations to study particle and Poynting energy fluxes and conclude how the ionospheric *E*- and *F*-regions are heated.

2. February 1, 2002 Cusp Event

[7] On 1 February 2002, Cluster and EISCAT radar in Svalbard (Longyearbyen, 78°N, 16°E) simultaneously observed the cusp on closely connected field lines. During the time interval of interest (12:00–12:30 UT), the ACE satellite observes variable IMF. In the first half of this time interval, IMF has the average values $B_x \sim 5$ nT, $B_y \sim -5$ nT, and $B_z \sim 5$ nT. In the second half of the interval more pronounced changes in IMF occur - B_x drops to 0 nT, B_y increase to -10 nT, and B_z momentarily becomes 0 and decreases to ~ -8 nT. The ACE IMF observations were accordingly lagged for the solar wind convection. Cluster was located at around 9 R_e altitude at the tail lobe side of the high-altitude cusp. Cluster's closest magnetic conjunction with EISCAT occurred around 12:00 UT (Figures 1a and 1b).

3. EISCAT/Cluster Observations

[8] On the ground, EISCAT observed the cusp for several hours from around 9:00 to 14:00 UT. The UHF 42 m antenna at Svalbard is directed in the magnetic field-aligned direction and probes the ionosphere in the range 90–1000 km. The radar spectrograms show enhanced electron density, and elevated electron and ion temperatures (Figures 2a–2c).

[9] The estimated energy flux in the *F*-region of the ionospheric cusp is shown in Figure 2d. The energy flux is derived calculating the cooling rates of the electrons due to elastic and inelastic processes, like Coulomb collisions of electrons with ambient ions; rotational and vibrational excitations of molecular neutrals; fine structure excitation and excitation of the lowest electronic state of the atomic oxygen, etc., [*Schunk and Nagy*, 2000]. The cooling rates depend on the densities of the particles, their temperatures and collisional frequencies. The electron density, and electron and ion temperatures, are provided by EISCAT. The neutral densities and temperatures are taken from MSIS-E-90 Atmosphere Model [*Hedin*, 1991]. The total effect of all collisional processes is estimated and the result is integrated over the altitudes from 250 to 600 km. The altitude range of integration is chosen so, because the heat exchange in the region due to soft particle precipitation is most effective there [*Kelley et al.*, 1982; *Millward et al.*, 1999].

[10] At high altitudes, Cluster was clearly in the exterior cusp from around 12:00 until 12:30 UT. The electron and ion spectrograms in Figures 3a and 3b, show high particle fluxes typical for the cusp. For the electrons the differential energy flux is $>10^9$ eV cm^{-2} s^{-1} sr^{-1} eV^{-1} in the energy range for 20 to 200 eV. For the ions, the flux is $\sim 10^8$ eV cm^{-2} s^{-1} sr^{-1} eV^{-1} in the range 200 to 1100 eV. The energy fluxes along the magnetic field are presented in

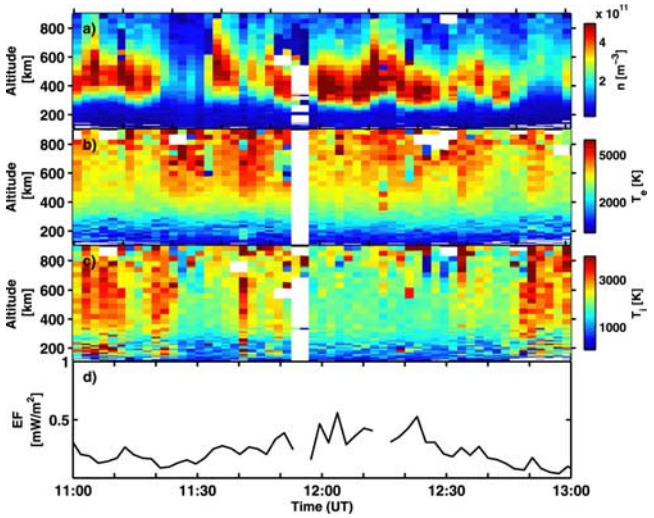

Figure 2. EISCAT observations: (a) electron density, (b) electron temperature, (c) ion temperature, and (d) energy flux (missing points are due to data gaps or uncertain EISCAT measurements).

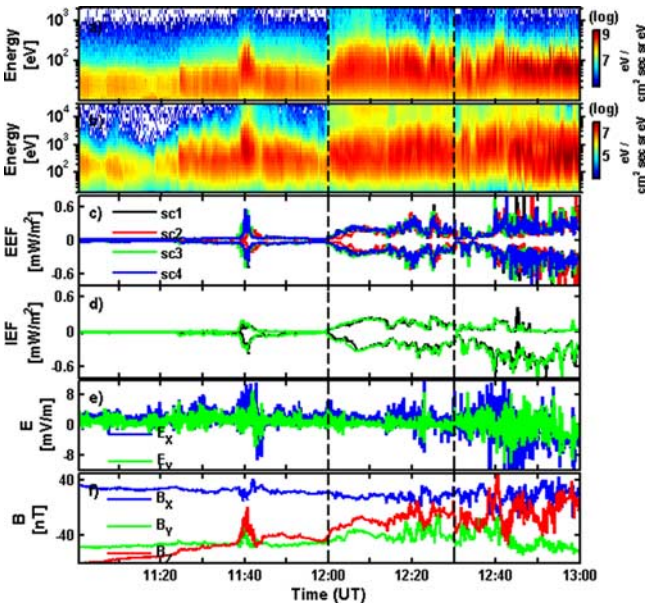

Figure 3. Cluster observations: (a) electron differential energy spectrogram (spacecraft 3), (b) ion differential energy spectrogram (spacecraft 3), (c) up- and downgoing (positive, earthward) electron energy flux (the different Cluster spacecraft correspond to different colours as seen from the legend), (d) up- and downgoing (positive, earthward) ion energy flux, (e) the GSE components (in colors) of the electric field (spacecraft 3), and (f) the GSE components (in colors) of the magnetic field (spacecraft 3). The dashed lines delimit the conjunction interval.

Figure 3c, for the electrons, and in panel *d*, for the ions. During this time interval, the magnetic field intensity, decreases in magnitude and varies strongly. Figure 3f presents the components of the magnetic field for spacecraft 3. The electric field, shows similar variable behavior (see the two components for spacecraft 3 in Figure 3e). There is a clear intensification of the fluctuations in all quantities observed by Cluster in the second half of the time interval probably due to the momentarily changes of the direction of IMF B_z component from Northward to Southward.

4. Results and Discussion

[11] We now concentrate on the time interval when Cluster and EISCAT are nearly conjugated in the cusp and estimate the total electromagnetic and particle energy fluxes entering the ionosphere. During the conjunction the field-aligned component of the Poynting flux $S_{||}$ as measured by Cluster is directed mainly earthward. $S_{||}$ was calculated from the two observed electric field components (almost perpendicular to the ambient $\mathbf{B}_0$) and the variations of the magnetic field obtained by subtracting a polynomial fit from the total field. On average the Poynting flux value is 0.012 mW/m^2. The convergence of the magnetic field (flux-tube scaling) implies that the ionosphere receives electromagnetic energy of about 12 mW/m^2. Next, we estimate the total particle energy flux at lower altitudes. For this purpose, one would like to determine the energy flux from the particles in the loss cone. Cluster particle instruments are unable to resolve the loss cone, which is less than 2 degrees. The small loss cone implies also that most of the earthward particles will mirror before reaching the ionosphere and will be observed at Cluster as particles going away from the earth. However, we can still estimate the total earthward particle energy flux at low ionospheric altitudes, assuming isotropy in the particle velocity distribution. The data are consistent with such an assumption. In this case, the particle energy flux at low ionospheric altitudes is the same as the total energy flux of all earthward particles at Cluster altitude. That is, it would be equal to the particle energy flux within the loss cone at Cluster altitude scaled by the flux-tube convergence. The average values of the total energy fluxes of the earthward going electrons and ions as measured by Cluster are 0.19 mW/m^2 and 0.15 mW/m^2, respectively (Figures 4b and 4c).

[12] Now we compare the energy fluxes of precipitating particles as estimated from Cluster and EISCAT measurements. The average energy input observed on EISCAT in the period 12:00–12:30 UT is about 0.4 mW/m^2 (Figure 4d, red curve), which is approximately equal to the total electron and ion energy flux estimated from Cluster (green and black curves, corresponding to the spacecraft 1 and 3). As discussed earlier, the particles observed by Cluster (Figures 3a and 3b) have low energies and therefore they will deposit their energy in the altitude range that is covered by EISCAT [*Kelley*, 1989]. Thus our experimental result suggests that the direct precipitation of the magnetosheath plasma into the ionosphere (no additional particle energiza-

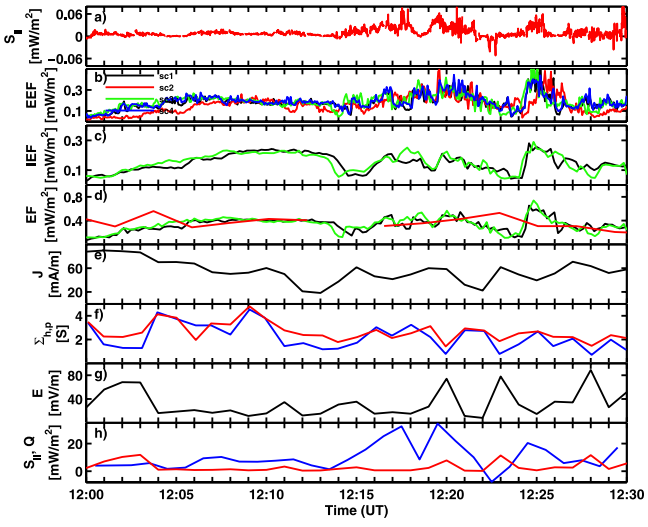

Figure 4. (a) The Poynting flux on Cluster (spacecraft 3) - positive toward the Earth; (b) downgoing electron energy flux (spacecraft 1–4); (c) downgoing ion energy flux (spacecraft 1 and 3); (d) total particle energy flux (spacecraft 1 and 3) and EISCAT energy input (red); (e) equivalent ionospheric current density (MIRACLE); (f) height-integrated Pedersen (red) and Hall conductivities (EISCAT) (blue); (g) ionospheric electric field strength; (h) the 1-minute averaged Poynting flux (blue), projected to the ionosphere and the Joule heating (red).

tion on the way to the ionosphere is required) is responsible for the *F*-layer heating.

[13] We now turn our attention to the Poynting flux and try to estimate how much of the electromagnetic energy is dissipated at low altitudes. To this end, we estimate the Joule heating in the ionosphere. To calculate the Joule heating, one needs to know the ionospheric electric field and conductivity. For this event, it was difficult to derive 2-D electric field only from the Svalbard 32 m antenna data. Instead, we calculated the electric field from the equivalent ionospheric current ($\mathbf{J_{eq,ion}}$). The current density (Figure 4e) is obtained using the technique of 2D upward continuation, introduced by [*Amm and Viljanen*, 1999], using a spatially extended network of magnetometer stations MIRACLE (Figure 1b). We assume that $\mathbf{J_{eq,ion}} = \mathbf{J_{Hall}}$, and that there are no gradients in the ionospheric conductivities. Both Pedersen and Hall height-integrated conductivities shown in Figure 4f, are derived from EISCAT measurements. The calculated electric field $E = J_{eq,ion}/\Sigma_h$, is presented in Figure 4g. With this in hand, we derived the Joule heating ($Q = E^2\Sigma_p$) in the *E*-layer of the ionosphere (Figure 4h, red curve). The average estimate of the Joule heating during this time interval is 3 mW/m^2. The projected to the ionosphere 1-minute averaged Poynting flux (blue curve) is 3 times higher. However, for some instants in the interval 12:15–12:22 UT, the Poynting flux reaches 10 times higher values. This clearly shows, that enough Poynting flux is seen at Cluster to explain the estimated large scale Joule heating of the ionosphere. The actual Joule heating could be considerably larger due to small scale electric field variability [*Codrescu and Fuller-Rowell*, 1995] and conductivity gradients. Part of the Poynting flux not being dissipated as Joule heating can either be reflected [*Streltsov and Lotko*, 2003] or cause other phenomena, e.g., particle acceleration along the field lines [*Wright et al.*, 2003; *Chaston et al.*, 2005].

5. Conclusions

[14] In this paper we have used the first conjugated ionospheric (EISCAT, MIRACLE) and high-altitude (Cluster) cusp observations to study the energy deposition into the ionosphere. EISCAT incoherent radar measurements of the plasma heating in the *F*-region (250–600 km) allowed us to estimate the energy input into this region. High altitude Cluster observations show that the earthward energy flux of particles with energies from tens to several hundred eV, closely matches the energy flux required to heat the *F*-region. Our experimental results suggest that the direct precipitation of the magnetosheath plasma into the ionosphere is responsible for the *F*-region heating. These results support earlier theoretical estimates and indirect observations.

[15] Estimates of the electric field and the conductivity give the Joule heating in the *E*-region (100–150 km). Cluster observations of the earthward Poynting flux, mapped to the ionosphere, is higher than what is needed to heat the *E*-region. This suggests that part of the Poynting flux heats the *E*-region, while the rest can go to the Joule heating at smaller scales than resolved in this work, or can be reflected, or lost along the flux-tube due to local wave-particle interactions.

[16] As a conclusion, we have shown that the particles seen at about 9 R_e in the exterior cusp carry an earthward energy flux that corresponds to the observed heating of the *F*-region. The earthward Poynting flux is more than enough to account for the Joule heating in the *E*-region.

[17] **Acknowledgments.** E. Yordanova would like to thank Andris Vaivads for the inspiring discussions and hints, and Alessandro Retinó for his assistance in dealing with some of the Cluster data. D. Sundkvist research was supported by NASA grant NNG05GL27G. We are indebted to the director and staff of EISCAT for operating the facility and supplying the data. EISCAT is an international association supported by Finland (SA), France(CNRS), Germany (MPG), Japan (NIPR), Norway (NFR), Sweden (VR), and the United Kingdom (PPARC). We also thank the ACE Science Center for providing the ACE data.

References

Amm, O., and A. Viljanen (1999), Ionospheric distrurbance magnetic field continuation from the ground to the ionosphere using spherical elementary current systems, *Earth Planets Space*, *51*, 431–440.

Amm, O., et al. (2005), Coordinated studies of the geospace environment using Cluster, satellite and ground-based data: An interim review, *Ann. Geophys.*, *23*, 2129–2170, sref:1432-0576/ag/2005-23-2129.

Chaston, C. C., et al. (2005), Energy deposition by Alfvén waves into the dayside auroral oval: Cluster and FAST observations, *J. Geophys. Res.*, *110*, A02211, doi:10.1029/2004JA010483.

Codrescu, M. V., and T. J. Fuller-Rowell (1995), On the importance of E-field variability for Joule heating in the high-latitude thermosphere, *Geophys. Res. Lett.*, *22*, 2393–2396.

Dunlop, M. W., et al. (2005), Cluster observations of the cusp: Magnetic structure and dynamics, *Surv. Geophys.*, *26*, 5–55.

Escoubet, C. P., R. Schmidt, and M. L. Goldstein (1997), Cluster—Science and mission overview, *Space Sci. Rev.*, *79*, 11–32.

Hedin, A. E. (1991), Extension of the MSIS thermosphere model into the middle and lower atmosphere, *J. Geophys. Res.*, *96*, 1159–1172.

Kelley, M. C. (1989), *The Earth's Ionosphere: Plasma Physics and Electrodynamics*, Elsevier, New York.

Kelley, M. C., J. F. Vickrey, C. W. Carlson, and R. Torbert (1982), On the origin and the spatial extent of high-latitude *F* region irregularities, *J. Geophys. Res.*, *87*, 4469–4475.

Korth, H., B. J. Anderson, H. U. Frey, and C. L. Waters (2005), High-latitude electromagnetic and particle energy flux during an event with sustained strongly northward IMF, *Ann. Geophys.*, *23*, 1295–1310.

Lavraud, B., et al. (2005), Cluster observes the high-altitude cusp region, *Surv. Geophys.*, *26*, 135–175.

Lockwood, M., et al. (2001), Coordinated Cluster, ground-based instrumentation and low-altitude satellite observations of transient poleward-moving events in the ionosphere and in the tail lobe, *Ann. Geophys.*, *19*, 1589–1612.

Lühr, H., M. Rother, W. Köhler, P. Ritter, and L. Grunwaldt (2004), Thermospheric up-welling in the cusp region: Evidence from CHAMP observations, *Geophys. Res. Lett.*, *31*, L06805, doi:10.1029/2003GL019314.

Millward, G. H., R. J. Moffett, and H. F. Balmforth (1999), Modeling the ionospheric effects of ion and electron precipitation in the cusp, *J. Geophys. Res.*, *104*, 24,603–24,612.

Nilsson, H., M. Yamauchi, L. Eliasson, and O. Norberg (1996), Ionospheric signature of the cusp as seen by incoherent scatter radar, *J. Geophys. Res.*, *101*, 10,947–10,963.

Prölss, G. W. (2006), Electron temperature enhancement beneath the magnetospheric cusp, *J. Geophys. Res.*, *111*, A07304, doi:10.1029/2006JA011618.

Schunk, R. W., and A. F. Nagy (2000), *Ionospheres: Physics, Plasma Physics, and Chemistry*, Cambridge Univ. Press, New York.

Streltsov, A. V., and W. Lotko (2003), Reflection and absorption of Alfvénic power in the low–altitude magnetosphere, *J. Geophys. Res.*, *108*(A4), 8016, doi:10.1029/2002JA009425.

Syrjäsuo, M., et al. (1998), Observations of substorm electrodynamics using the MIRACLE network, in *Substorms-4: International Conference on Substorms-4, Lake Hamana, Japan, March 9–13*, edited by S. Kokubun and Y. Kamide, Terra Sci. Pub., Tokyo.

Walker, I. K., J. Moen, L. Kersley, and D. A. Lorentzen (1999), On the possible role of cusp/cleft precipitation in the formation of polar-cap patches, *Ann. Geophys.*, *17*, 1298–1305.

Wright, A., W. Allan, and P. A. Damiano (2003), Alfvén wave dissipation via electron energization, *Geophys. Res. Lett.*, *30*(16), 1847, doi:10.1029/2003GL017605.

Wu, Q., T. L. Killeen, W. Deng, A. G. Burns, J. D. Winningham, N. W. Spencer, R. A. Heelis, and W. B. Hanson (1996), Dynamics Explorer 2 satellite observations and satellite track model calculations in the cusp/cleft region, *J. Geophys. Res.*, *101*, 5329–5342.

O. Amm, Space Physics, Finnish Meteorological Institute, P.O. Box 503, FIN-00101 Helsinki, Finland.

M. André, S. C. Buchert, M. Morooka, and E. Yordanova, Space Plasma Physics, Swedish Institute of Space Physics, Box 537, SE-75121 Uppsala, Sweden. (eya@irfu.se)

A. N. Fazakerley, Space Plasma Physics, Mullard Space Science Laboratory, Holmbury St. Mary, Dorking RH5 6NT, UK.

O. Margithu, Space Research Laboratory, Institute of Space Sciences, P.O. Box MG-23, Ro 76900, Bucharest-Magurele, Romania.

Y. Ogawa, Space and Upper Atmospheric Science, National Institute of Polar Research, 9-10 Kaga 1-chome, Tokyo 173-8515, Japan.

H. Réme, Systeme Solaire, CESR, 9 avenue du Colonel Roche, F-31028 Toulouse, France.

D. Sundkvist, Space Sciences Laboratory, University of California, 7 Gauss Way, Berkeley, CA 94720-7450, USA.